

# Leading interactions in the $\beta$ - $SrV_6O_{15}$ compound

Marie-Liesse Doublet<sup>1</sup> and Marie-Bernadette Lepetit<sup>2</sup>

<sup>1</sup>*Laboratoire de Structure et Dynamique des Systèmes Moléculaires et Solides,  
LSDSMS / UMR 5636, Université Montpellier 2,  
Place Eugène Bataillon, F-34095 Montpellier Cedex 5, FRANCE*

<sup>2</sup>*Laboratoire de Physique Quantique, IRSAMC / UMR 5626, Université Paul Sabatier,  
118 route de Narbonne, F-31062 Toulouse Cedex 4, FRANCE\**

(Dated: February 7, 2022)

The present study shows that the electronic structure of the  $\beta$ - $AV_6O_{15}$  family of compounds ( $A = Sr, Ca, Na...$ ) is based on weakly interacting two-leg ladders, in contrast with the zig-zag chain model one could expect from their crystal structure. Spin dimer analysis, based on extended Hückel tight-binding calculations, was performed to determine the structure of the dominant transfer and magnetic interactions in the room temperature  $\beta$ - $SrV_6O_{15}$  phase. Two different two-legs ladders, associated with different charge/spin orders are proposed to describe these one-dimensional  $\beta$ -type systems. The antiferromagnetic ladders are packed in an 'IPN' geometry and coupled to each other through weak antiferromagnetic interactions. This arrangement of the dominant interactions explains the otherwise surprising similarities of the optical conductivity and Raman spectra for the one-dimensional  $\beta$ -type phases and the two-dimensional  $\alpha$ -type ones such as the well-known  $\alpha'$ - $NaV_2O_5$  system.

## I. INTRODUCTION

Vanadium oxides are known since the fifties but they have attracted a lot of attention in the recent years because of their exotic behavior. Their remarkable properties are due to the interplay between charge, spin and lattice degrees of freedom. One of the most famous example is the  $\alpha'$ - $NaV_2O_5$  phase that undergoes a spin-Peierls transition<sup>1</sup> coupled to a spin ordering. This double transition has raised a large controversy in the last five years before its nature and origin could be elucidated, and before the apparent experimental contradictions could be lifted. Indeed, the ordering associated with the transition was supposed to be a charge ordering of the vanadium unpaired electron, located on each rung of this two-legs ladder system<sup>2</sup>. While vanadium NMR<sup>3</sup> and neutron diffraction<sup>4</sup> experiments exhibited a large charge ordering at the transition, optical conductivity<sup>5</sup> and resonant X-ray diffraction<sup>6</sup> did not show much charge ordering. The controversy was lifted when ab-initio calculations<sup>7</sup> showed that i) the bridging oxygens of the ladder rungs have an open-shell character, ii) there are three and not one magnetic electron per ladder rung and thus spin and charge densities are not compelled to be equal, iii) the system presents a large spin ordering (seen by spin sensitive experiments) associated with a very weak charge ordering (as observed in charge sensitive experiments).

Recently, superconductivity has been discovered in another family of vanadium bronzes, renewing the interest in low-dimensional vanadium oxides. The different phases of the  $\beta$ - $AV_6O_{15}$  ( $A = Li, Na, Ag, Ca, Sr, Cu$ ) family, also referred to as  $\beta$ - $A_{0.33}V_2O_5$ , exhibit an one-dimensional (1D) metallic behavior at room temperature and undergo a metal to insulator phase transition at  $T_{MI}$ <sup>8</sup>, associated with a charge ordering. Systems with monovalent cations ( $A^+$ ) show a long-range magnetic order at  $T < T_{MI}$ <sup>9</sup>. In systems with divalent cations ( $A^{2+}$ ),

no sign of long-range magnetic order is observed down to 2K and a spin gap appears in  $SrV_6O_{15}$ <sup>10</sup>. The  $\beta$ -type phases present crystal structures with a 1D arrangement along the  $b$  direction — unlike the layered character of the  $\alpha$ -type phases. They show six crystallographically independent vanadium atoms two-by-two distributed over different cationic sites : two  $V_1$  atoms that form zig-zag double chains composed of edge-sharing  $VO_5$  square-based pyramids, two  $V_2$  atoms that form two-leg ladders composed of  $V_2O_5$  square-based pyramid sharing a corner with  $V_{2a}O_6$  distorted octahedron, and two  $V_3$  atoms that form zig-zag edge-sharing double chains, similar to the  $V_1$ 's, at first sights.

Some remarks should be done at this point.

First, in the  $\beta$ -type systems, phases with remarkable similitude of their structural arrangements, whether they are doped by mono- or divalent cations, exhibit very different magnetic properties. Ueda *et al*<sup>10</sup> suggested that the differences in the magnetic properties are due to the different nature of the electronically dominant subsystem. The electronically dominant subsystem would be the zig-zag chains in the  $\beta$ - $A^+V_6O_{15}$  and ladders in  $\beta$ - $A^{2+}V_6O_{15}$  compounds.

Second, the  $\alpha$  and  $\beta$  compounds have very different structural arrangements — the former is 2D while the latter is 1D — however their spectroscopic properties such as Raman<sup>11</sup> and optical conductivity spectra<sup>12</sup> show remarkable similitudes.

A simple formal charge analysis gives  $A^+V_6^{(5-1/6)+}O_{15}^{2-}$  for monovalent cations and  $A^{2+}V_6^{(5-1/3)+}O_{15}^{2-}$  for divalent cations. It comes a filling of either one or two 3d electrons for 6 vanadium atoms. This (low) filling, as well as the strongly localized character of the first row transition metal 3d orbitals, justify the use of a  $t - J$  model on the vanadium sites to describe the low energy physics of such vanadates.

The present paper thus aims at elucidating the structure of the dominant electronic interactions in the  $\beta$ -type compounds within the hypothesis of a  $t - J$  model. For this purpose, spin dimer analysis was performed using extended-Hückel tight-binding (EHTB) electronic structure calculations. Since  $\beta$ - $AV_6O_{15}$  unit cells consist in (at least) four formula units, *i.e.* 88 atoms, this approach offers a pertinent alternative to prohibitive *ab initio* calculations. Furthermore, the EHTB method has been shown to provide reliable and expedient means to study the relative strengths of both hopping and spin exchange interactions in a wide variety of transition metal oxides<sup>13</sup>. Because strongly interacting spin exchange paths of a magnetic solid are determined either by the overlap between its magnetic orbitals for non-bridged interactions, or by the overlap between its magnetic orbitals and the bridging ligand orbitals for bridged interactions, a qualitative picture of both the dominant magnetic interactions and their nature (antiferromagnetic versus ferromagnetic) is reachable using EHTB, provided the knowledge of the crystal structure. In the present work, calculations have been performed using the crystallographic data reported for the  $\beta$ - $SrV_6O_{15}$  compound<sup>14</sup>.

## II. STRUCTURE OF THE DOMINANT INTERACTIONS

In the  $\beta$ -type compounds, five of the six vanadium atoms are surrounded by five nearest-neighbor (NN) oxygen atoms forming a distorted squared pyramid ( $V_{1a}$ ,  $V_{1b}$ ,  $V_{2b}$ ,  $V_{3a}$  and  $V_{3b}$ ). A sixth oxygen neighbor is found at a larger distance in the position issued from a highly distorted  $VO_6$  octahedron (see figure 1). For the sixth vanadium atom  $V_{2a}$ , a less marked pyramidal structure is observed, with two short, two medium and two long  $V - O$  bonds. Each pyramid may actually be seen as a

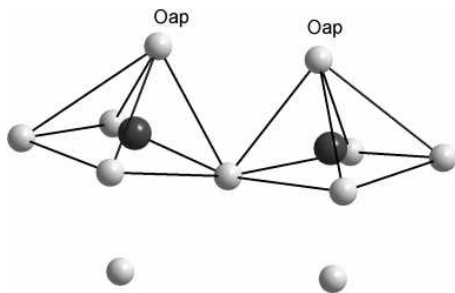


FIG. 1: Local environment of vanadium atoms in the  $\beta$ - $AV_6O_{15}$  phases. Vanadium and oxygen atoms correspond to dark and light gray spheres, respectively.

vanadyl  $V \equiv O_{ap}$  cation lying above a distorted square of  $O^{2-}$  anions. Indeed, the  $V-O_{ap}$  distance is much smaller ( $\sim 1.6\text{\AA}$ ) than the  $V-O$  distances involving either the oxygens contained in the pyramid basal plane ( $\sim 1.9\text{\AA}$ – $2.0\text{\AA}$ ), or the sixth oxygen ( $\sim 2.3\text{\AA}$ ). Let us note that the  $V \equiv O_{ap}$  cations are not rigorously perpendicular to the

basal plane of the pyramids. The existence of an apical oxygen is crucial in these systems since the short  $V-O_{ap}$  distance allows a strong delocalization to occur between these two atoms and a multiple vanadium–oxygen covalent bond to take place. This phenomenon has already been observed in the  $\alpha'$ - $NaV_2O_5$  compound, in which a triple covalent/dative bond exists between the vanadium and its apical oxygen. This bond is only weakly polarized<sup>15</sup> with an oxygen charge of about  $-0.5$ . The experimental signature of such a strong multiple bond in the Raman spectra is a sharp peak at relatively high energy, corresponding to the bond stretching mode. This peak occurs at  $969\text{cm}^{-1}$  for the  $\alpha'$ - $NaV_2O_5$ <sup>16</sup>, at  $932\text{cm}^{-1}$  and  $1002\text{cm}^{-1}$  for the  $CaV_2O_5$  and  $MgV_2O_5$ <sup>17</sup> respectively. In the  $\beta$ - $CaV_6O_{15}$ <sup>11</sup>, it is seen at  $978\text{cm}^{-1}$ ,  $952\text{cm}^{-1}$  and  $877\text{cm}^{-1}$  for the  $V_3$ ,  $V_1$  and  $V_2$  vanadyl bonds. Note that the softening of the apical bond stretching mode for the  $V_2$  atoms is due to a less marked pyramidal character of its oxygen first neighbors.

Two consequences arise from the occurrence of such a  $V-O_{ap}$  multiple bond. First the formal charge of the vanadium atom is much smaller than what is usually assumed. It should be accounted as  $5 - \eta - q$  instead of  $5 - \eta$  where  $\eta$  is the number of magnetic  $3d$  electrons per vanadium atom and  $q$  is the number of vanadium electrons participating to the vanadyl bond. Second and much more important, the vanadyl bond acts as a local quantification axis for the vanadium atom. As a consequence, the nature of the  $3d$  magnetic orbital can be deduced from the vanadyl bond orientation : it is the  $d_{xy}$  orbital, when local axes are chosen so that  $z$  is collinear to the vanadyl bond and  $x$  and  $y$  point toward the basal plane first oxygen neighbors (see figure 2). Indeed, while the  $d_{z^2}$ ,  $d_{xz}$  and  $d_{yz}$  vanadium orbitals form one  $\sigma$  and two  $\pi$  covalent/dative bonds with the apical oxygen, the  $d_{xy}$  and  $d_{x^2-y^2}$  orbitals are split in agreement with the crystal field. The  $d_{x^2-y^2}$  orbital is more destabilized than the  $d_{xy}$  one due to its  $\sigma$ -type overlap with the basal plane oxygen atoms which is larger than the  $\pi$ -type overlap of the  $d_{xy}$  orbital. Note that the structural difference observed for the  $V_{2a}$  local environment induces a lowering of one of the two anti-bonding  $\pi$ -orbitals close to the magnetic orbital energy and therefore a slightly different orientation of the  $V_{2a}$  magnetic orbital.

Focusing now on the orientation of the vanadium magnetic orbitals in the crystal structure, it becomes very simple to build the structure of the magnetic orbitals once each vanadyl bond is located. Figure 3 reports this structure for the  $\beta$ - $SrV_6O_{15}$  system. The existence of two sets of vanadium atoms can be clearly seen : on one hand the  $V_1$  and  $V_3$  centers for which the magnetic orbitals are roughly in the  $(c, b)$  plane and on the other hand the  $V_2$  centers for which the magnetic orbitals are nearly orthogonal to the previous ones, in the approximate  $(a + c, b)$  plane.

Let us now analyze separately each type of crystallographic chain or ladder. Figure 4 reports the relative position of the magnetic orbitals for the  $V_2$  ladder.

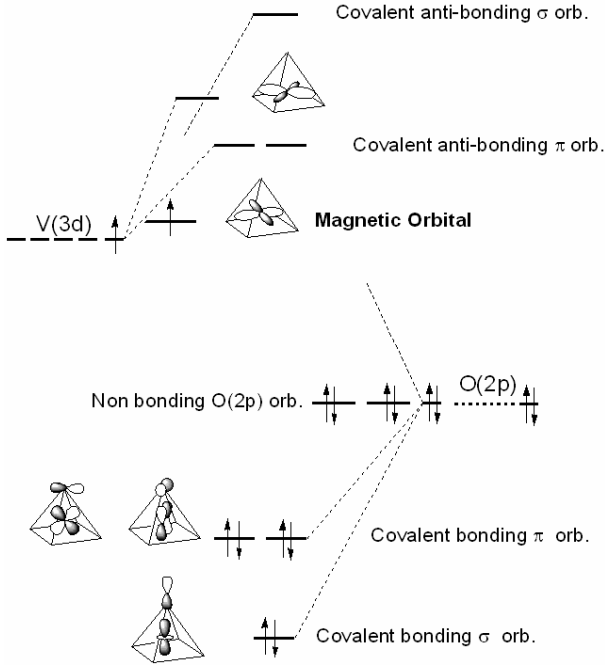


FIG. 2: Qualitative orbital interaction between the vanadium 3d orbitals and the  $p$  orbitals of the pyramid oxygens. The apical oxygen lies on the  $z$  axis, while the four oxygens of the pyramid basal plane lie on the  $x$  and  $y$  axes.

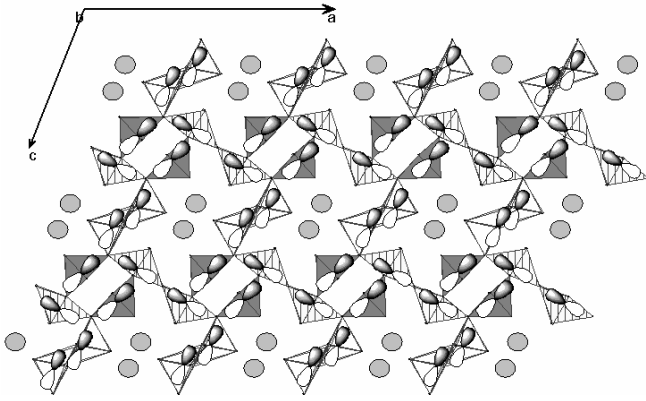


FIG. 3: Structural arrangement of the vanadium magnetic orbitals as derived both from the vanadyl bond orientation on each vanadium atom and from extended Hückel calculations. The crystal structure is represented within the  $(a, c)$  plane. The gray circles represent the counter ions, the  $V_2$  pyramids are hatched, the  $V_3$  are represented in white and the  $V_1$  in gray.

Let us note that vanadyl bonds are nearly orthogonal to the figure, pointing alternatively above and below the figure plane. The bridging-oxygen  $p_x$  orbitals, along the ladder legs, and  $p_y$  orbitals along the ladder rungs strongly overlap with the neighboring  $V_2$  magnetic orbitals. They will thus mediate both transfer and magnetic interactions. This qualitative description is con-

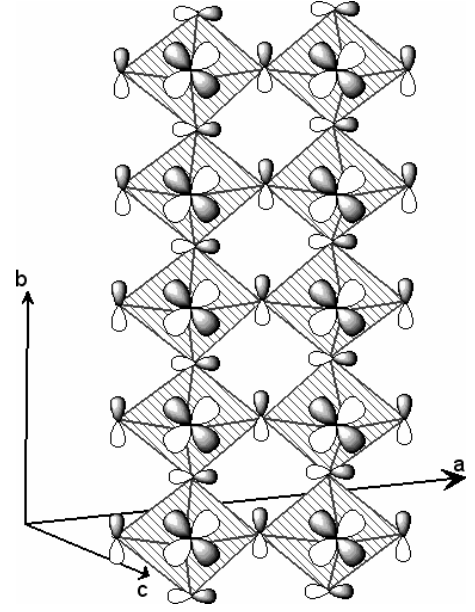


FIG. 4: Vanadium magnetic orbitals of a  $V_2$  ladder and  $p$  orbitals of the bridging oxygen atoms mediating the interactions between the former. Note that orbital signs do not have any meaning here. The local  $x$ ,  $y$  and  $z$  axes are defined as such : the  $z$  axis is in the  $V_2b$  vanadyl bond direction, the  $x$  axis is in the ladder rungs direction and the  $y$  axis along the  $b$  crystallographic direction.

firmed by spin dimer EHTB calculations since the largest spin exchange paths (*i.e.* the largest effective transfer integrals) occur between the  $V_2$  magnetic centers, as stacked in the two-leg ladder shown in figure 4. Due to significant local distortions of the  $V_2$ -centered pyramids, transfer integrals are larger along the ladder rungs ( $\sim 0.31$  eV) than along the ladder legs (0.17 eV and 0.21 eV). Nevertheless, both effective integrals are large enough to expect antiferromagnetic interactions between the  $V_2$  atoms. Indeed, the effective transfer mediated through the appropriate  $p$  orbital of the bridging oxygen, can be expressed as

$$t = \pm \frac{t_{pd}^2}{\Delta_1} \quad (1)$$

and thus the bridged super-exchange mechanism comes as

$$J = -4 \frac{t_{pd}^4}{(\Delta_1)^2 U_d} - 8 \frac{t_{pd}^4}{(\Delta_1)^2 \Delta_2} \quad (2)$$

$$= -4 \frac{t^2}{U_d} - 8 \frac{t^2}{\Delta_2} \quad (3)$$

with  $\Delta_1 = \delta - U_p + U_d - V_{pd}$  and  $\Delta_2 = 2\delta - U_p + 2U_d - 4V_{pd}$ .  $\delta$  is the orbital energy difference between the vanadium magnetic orbital and the bridging oxygen  $p$  orbital,  $t_{pd}$  is the transfer integral between them,  $U_p$  and  $U_d$  are the on-site Coulomb repulsions and  $V_{pd}$  is the bi-electronic repulsion between the V and O orbitals.

Figure 5 reports the relative position of the magnetic orbital for the  $V_1$  zig-zag chains. One sees immediately

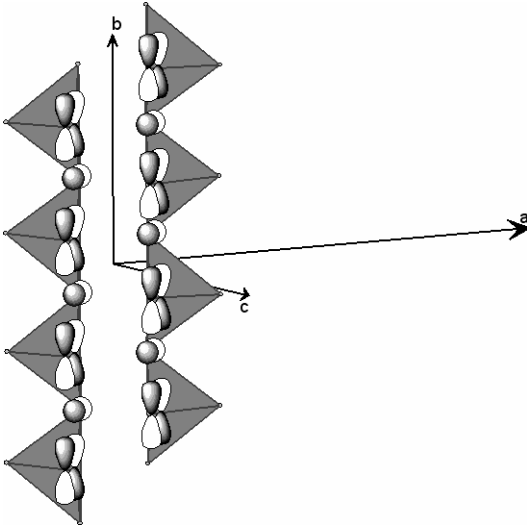


FIG. 5: Magnetic orbitals of the  $V_1$  zig-zag chains and  $p$  orbitals of the bridging oxygen atoms involved in the mediation of the  $V_1$  magnetic orbitals interaction. Note that the orbitals represented here are atomic orbitals and that the relative phases between them do not have any meaning. Local  $x$ ,  $y$  and  $z$  axes are defined as such :  $z$  is in the vanadyl bonds direction,  $y$  is along the  $b$  crystallographic direction and  $x$  is orthogonal to the formers.

that the hopping between the magnetic orbitals of two nearest neighbors (NN)  $V_1$  atoms is not bridged by any oxygen orbital that could mediate the interaction, and is thus restricted to its direct contribution. This direct contribution is itself expected to be very small, due to both the large distance between adjacent  $V_1$  atoms ( $\sim 3.3\text{\AA}$ ) and the  $\delta$  character of the overlap. EHTB calculations confirm these remarks since the transfer integral between NN  $V_1$  magnetic orbitals is found to be negligible. As far as the magnetic exchange is concerned, no super-exchange mechanism can take place between the NN  $V_1$  atoms, for the same reasons. Therefore, the effective magnetic interaction is reduced to the direct exchange between the two vanadium atoms. It can thus be predicted to be very weak and ferromagnetic. One can clearly consider that the NN  $V_1$  atoms do not interact. Let us now examine the coupling between second neighbor  $V_1$  atoms. One sees on figure 5 that the associated pyramids share a corner in the  $b$  direction and that the  $p_x$  orbital of the bridging oxygen presents a large overlap with the vanadium magnetic orbitals. It can thus mediate efficiently the interaction between second neighbor  $V_1$  atoms. EHTB calculations yield effective transfer integrals of  $0.17\text{ eV}$  and  $0.15\text{ eV}$ . Through-bridge super-exchange mechanism should take place and the effective exchange between second neighbor  $V_1$  atoms can thus be expected to be reasonably large and antiferromagnetic.

Figure 6 reports the relative position of the magnetic

orbitals of both the  $V_1$  and  $V_3$  chains. The magnetic

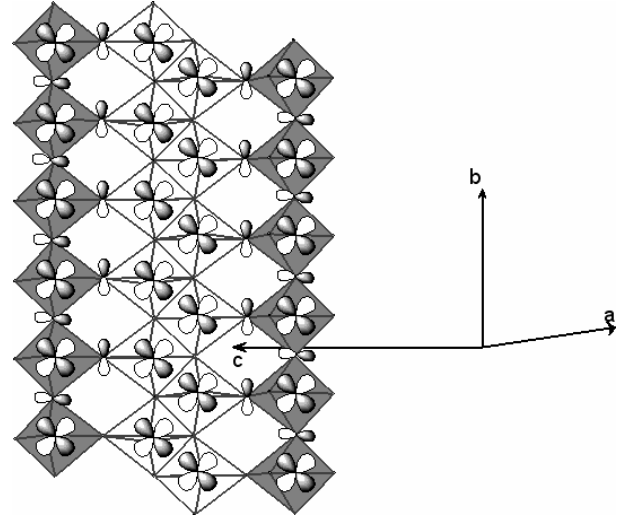


FIG. 6: Magnetic orbitals of the  $V_1$  and  $V_3$  chains along the  $b$  direction and  $p$  orbitals of the bridging oxygen atoms. Note that the orbitals represented here are atomic orbitals and that the relative phases between them do not have any meaning. Pyramids associated with the  $V_1$  and  $V_3$  atoms are represented in gray and white, respectively. Local  $x$ ,  $y$  and  $z$  axes are defined as such :  $z$  is in the vanadyl bonds direction which is orthogonal to the figure plane,  $y$  is along the  $b$  crystallographic direction and  $x$  is orthogonal to the formers.

orbitals of the  $V_3$  zig-zag chains are similar to the magnetic orbitals of the  $V_1$  atoms since the apical axes of both sets of atoms are along the same direction. The  $V_3$  pyramids share an edge and the interaction between the  $V_3$  magnetic orbitals is bridged by two oxygen atoms with nearly  $90^\circ$   $V_3\text{-O-}V_3$  angles. It is well known that in such  $90^\circ$  arrangements, the contribution of the bridging-oxygen  $p$  orbitals is destructive and that the interactions between the vanadium magnetic orbitals are restricted to the direct transfer and exchange integrals. These interactions are thus weak due to the large distance between two NN vanadium atoms ( $\sim 3.0\text{\AA}$ ). Indeed, EHTB calculations yield effective transfers between nearest neighbor  $V_3$  atoms of the order of  $\simeq 0.05\text{ eV}$  (see Appendix for the exact values of the four crystallographically different  $V_3\text{-}V_3$  transfer integrals). As far as the effective exchange is concerned, one can expect it to be both weak (of the order of a few tenth of meV or smaller) and ferromagnetic — the direct exchange is always ferromagnetic in nature. Let us now examine the second neighbor  $V_3\text{-}V_3$  interactions. The associated pyramids share a corner along the  $b$  direction and the  $p_x$  orbital of the oxygen atom (not shown on figure 6) can efficiently mediate the interactions between two vanadium atoms. EHTB calculations yield transfer integrals of  $0.14\text{ eV}$ . Through-bridge super-exchange mechanism takes place via the oxygens  $p_x$  orbitals and the effective exchange between second neighbors  $V_3$  atoms should thus be reasonably large (hundreds of meV) and antiferromagnetic.

It is clear from figure 6 that there is another type of large vanadium-vanadium interactions that is not considered in the literature, that is the  $V_1$ - $V_3$  interaction. Indeed, the NN  $V_1$  and  $V_3$  magnetic orbitals are bridged by a  $p_y$  oxygen orbital that mediates the interactions between them. EHTB calculations confirm the present remarks with an evaluation of the transfer integral of 0.20 eV and 0.23 eV. Of course this  $p_y$  oxygen orbital will mediate a super-exchange mechanism so that the magnetic interaction can be expected to be large and antiferromagnetic.

Summarizing the above results, one sees that the structure of the dominant interactions, both transfer and magnetic, does not follow the crystallographic zig-zag chains structure. Actually, the dominant interactions are arranged in two types of two-leg ladders, namely the  $V_2$ - $V_2$  ladders and the  $V_1$ - $V_3$  ladders which are crystallographically orthogonal to each other. The average filling of these ladders is of one electron for 3 sites in systems doped with divalent cations and of one electron for 6 sites in systems doped with monovalent cations. All magnetic interactions within these ladders show an antiferromagnetic character.

Let us now analyze the interactions between these ladders. The coupling between two  $V_1$ - $V_3$  ladders could go either through  $V_1$ - $V_1$  NN interactions which we have seen to be totally negligible, both in terms of electron transfer and magnetic interactions, or through the  $V_3$ - $V_3$  NN interactions. The latter are somewhat larger than the NN  $V_1$ - $V_1$  interactions but still quite weak and ferromagnetic in character.

Are there other types of inter-ladder interactions? Going back to figure 3, one sees that the  $V_1$ ,  $V_2$  and  $V_3$  pyramids share a corner.

Let us note the local axes in the following manner :  $y$  for the  $b$  direction,  $x$  and  $z$  in such a way that the  $V_1$  and  $V_3$  magnetic orbitals are  $d_{xy}$  and the  $V_2$  magnetic orbitals are  $d_{zy}$  in nature.

The  $p_y$  orbitals of the  $V_1$ - $V_2$ - $V_3$  bridging oxygen mediates the  $V_1$ - $V_3$  interaction. One should notice that despite the nearly  $90^\circ$   $V_1$ -O- $V_2$  and  $V_3$ -O- $V_2$  angles, the oxygen  $p_y$  orbital can efficiently mediate the transfer interaction between i) the  $V_1$  and  $V_2$  magnetic orbitals and ii) the  $V_3$  and  $V_2$  magnetic orbitals. This is due to the fact that, unlike the classical case, the  $V_n$  magnetic orbitals are orthogonal to the  $(V_1, O, V_2)$  and  $(V_3, O, V_2)$  planes. Indeed, EHTB calculations yield  $V_1$ - $V_2$  and  $V_3$ - $V_2$  transfer integrals of the order of 70 meV and 25 meV. As far as the magnetic exchange is concerned, the  $p_y$  orbital is able to mediate super-exchange mechanism. Thus the effective exchange between the  $V_1$ - $V_3$  and  $V_2$ - $V_2$  ladders i) goes through the local  $V_1$ - $V_2$  and  $V_3$ - $V_2$  interactions, ii) can be expected to be weak but much larger than the exchange between two  $V_1$ - $V_3$  ladders and iii) is antiferromagnetic in character.

In conclusion one can see the  $\beta$ - $AV_6O_{15}$  compounds as composed of two types of orthogonal two-legs ladders packed in an 'IPN' geometry (see figure 7) and coupled

through antiferromagnetic exchange interactions.

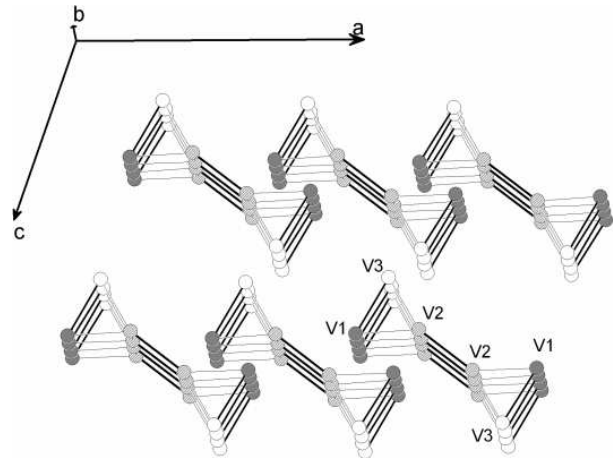


FIG. 7: Structure of the dominant interactions in the  $\beta$ - $AV_6O_{15}$  compounds. Strong intra-ladder interactions are in dark gray, while inter-ladder interaction are pictured in light gray.

### III. ON SITE ENERGIES

In the  $\beta$ - $AV_6O_{15}$  compounds, the ladder rungs are built on two crystallographically different vanadium atoms. This is obviously the case for the  $V_1$ - $V_3$  ladders and often for the  $V_2$ - $V_2$  ladders. For instance, even in the high temperature phase, the  $Sr$  and  $Ca$  compounds present a dimerization along the  $b$  direction so that the  $V_2$ - $V_2$  ladder rungs are composed of  $V_{2a}$  and  $V_{2b}$  crystallographically different atoms. These crystallographic differences, which are system and phase specific, are due to different chemical parameters such as the size of the  $A^{n+}$  cation, its location (in the  $\beta$  or  $\beta'$  sites), or the electronic instabilities toward spin-Peierls type of distortion. The consequence of these characteristics is that the energies of the two vanadium magnetic orbitals in one ladder rung are different. EHTB calculations show that these energy differences are not negligible, even in the high temperature phases, since they can reach values as large as 0.18 eV on the  $V_2$ - $V_2$  ladders. Surprisingly the  $V_1$ - $V_3$  ladders are much more symmetric with an orbital energy difference between the  $V_1$  and  $V_3$  magnetic orbitals of 0.05 eV only.

The first consequence is that there should be a charge/spin order, even in the high temperature phases. The second one is that the average fillings,  $\eta_{13}$  and  $\eta_{22}$ , of the two types of ladders have no reason to be equal and that a charge transfer degree of freedom between the two ladders should be taken into account.

#### IV. THE LOW TEMPERATURE PHASE

Similar EHTB calculations as those detailed in the preceding sections were done on the low temperature phase (LTPh). Structural data at 90K were taken from reference<sup>14</sup>. In the low temperature phase the unit cell is tripled along the ladder axis  $b$ . Sellier *et al* attributed this  $3 \times b$  super-cell to small displacements of the  $V_2$  atoms within the  $V_2$  ladders rungs.

As expected, the results in the LTPh exhibit on-site orbital energies and transfer integral modulations compared to the high temperature phase (HTPh), however the main conclusions remain unchanged. Indeed, as in the HTPh, the dominant interactions are arranged in antiferromagnetic ladders, and these ladders are then antiferromagnetically coupled according to an IPN geometry. The main difference between the two phases is that while in the HTPh the transfer between IPNs is always very small, in the LTPh some of the  $V_3$ - $V_3$  transfers are of the same order of magnitude as the intra-IPN ones. Another point to be noticed is that the variation range of the on-site orbital energies along the ladders is larger in the LTPh than in the HTPh. These differences can thus be expected to induce a greater electron localization in the ladder direction (in agreement with the observed metal to insulator transition) and a somewhat lesser 1D character in the LTPh.

#### V. DISCUSSION AND CONCLUSION

One of the troubling properties of the  $\beta$ - $AV_6O_{15}$  compounds is that, while their crystallographic structure is very different from that of the  $\alpha'$ - $NaV_2O_5$  system, they present very similar features, both in the optical conductivity and Raman spectra. The present study partially explains these similarities. Indeed, the electronic structures of the two compounds are based on similar units, despite their a-priori different crystallographic structures. They show (i) square-pyramid environment of the vanadium atoms with magnetic orbitals orthogonal to a very short vanadyl bond, and (ii) dominant interactions of the magnetic centers arranged in two-leg ladders with antiferromagnetic interactions.

The vanadyl multiple bond is responsible for the existence of a sharp peak around  $1000 \text{ cm}^{-1}$  in the Raman spectra of both  $\beta$  and  $\alpha$  compounds. Other features related to the existence of the pyramidal entities are present in the Raman spectra of both type of compounds such as the bending mode between two pyramids around  $440 \text{ cm}^{-1}$ . Finally, one retrieves in both compounds the broad feature in the  $550 \text{ cm}^{-1}$  to  $700 \text{ cm}^{-1}$  range that was attributed in the  $\alpha'$ - $NaV_2O_5$  to the electron-phonon coupling<sup>19</sup> responsible for the spin-Peierls transition.

The optical conductivity spectra for both the  $\beta$ - $AV_6O_{15}$  and the  $\alpha'$ - $NaV_2O_5$  compounds also present strong similitudes, such as the famous  $1 \text{ eV}$  peak. This peak was attributed in the  $\alpha'$ - $NaV_2O_5$  system to the first

doublet-doublet excitation energy on the ladder rung. It is also present in the  $\beta$ -type compounds, which are ladder systems, as well. In the  $SrV_6O_{15}$ , this peak is double ( $0.85 \text{ eV}$  and  $1.2 \text{ eV}$ <sup>12</sup>). In the assumption that this peak can also be attributed to the first doublet-doublet excitation energy of the ladder rungs, the doubling would be in total agreement with the electronic structure proposed in this work, namely two-leg ladders of two different types.

The occurrence of this peak in the  $\beta$ -type compounds raises several more general questions on 1D vanadium oxides.

- The first one is whether the existence of this  $1 \text{ eV}$  feature is the signature of a ladder arrangement of the dominant interactions in the vanadium oxides.
- It has been shown in the  $\alpha'$ - $NaV_2O_5$  compound that the ladder rung should not be seen as supporting one electron delocalized on the two vanadium magnetic orbitals, but rather three magnetic electrons, since the bridging oxygen shows a strong open-shell character and the local wave-function is multiconfigurational<sup>7,15</sup>.  
The second question is thus whether this magnetic character of the rung bridging oxygen is a general feature of the vanadium oxides with a two-leg ladders electronic structure.
- The third question is whether the  $1 \text{ eV}$  peak is the signature of this magnetic character of the rung oxygens. One of us is actually running ab-initio calculations in order to check these questions in the  $\beta$  compounds. The preliminary results confirm these hypotheses.

Finally let us remember that the sodium phase of the  $\beta$ - $AV_6O_{15}$  family presents a super-conducting phase. Put into perspective with the present results yielding a ladder structure for the dominant interactions, one can wonder whether this compound could be a realization of the predicted superconductivity in doped ladder systems<sup>20</sup>.

**Acknowledgments :** the authors thank the following research groups for helpful discussions, namely E. Janod, Cl. Sellier, and co-workers from the *Institut des matériaux Jean Rouxel*, V. Ta Phuoc from the *Laboratoire d'électrodynamique des matériaux avancés*, Y. Fagot-Revurat and co-workers from the *Laboratoire de Physique des Matériaux*. We also thank the Groupement de Recherche 2069 of the CNRS, *Oxydes à propriétés remarquables*, for having made this collaboration possible.

#### Appendix

V <sub>1</sub> -V <sub>3</sub> ladder					
Rungs			Legs		
Atoms	$t$	$\Delta\varepsilon$	Atoms	$t$	$\Delta\varepsilon$
V <sub>1b</sub> -V <sub>3b</sub>	-0.203	0.050	V <sub>1a</sub> -V <sub>1b</sub>	-0.173	0.00
V <sub>1a</sub> -V <sub>3a</sub>	-0.237	0.113	V <sub>1a</sub> -V <sub>1b+b</sub>	-0.145	0.00
			V <sub>3a</sub> -V <sub>3b</sub>	-0.148	-0.038
			V <sub>3a</sub> -V <sub>3b+b</sub>	-0.140	-0.040

---

V <sub>2</sub> -V <sub>2</sub> ladder					
Rungs			Legs		
Atoms	$t$	$\Delta\varepsilon$	Atoms	$t$	$\Delta\varepsilon$
V <sub>2a</sub> -V <sub>2b</sub>	-0.313	-0.184	V <sub>2a</sub> -V <sub>2b</sub>	-0.147	-0.173
			V <sub>2a</sub> -V <sub>2b+b</sub>	-0.135	0.215

---

Inter-ladder Intra-IPN					
Atoms	$t$	$\Delta\varepsilon$	Atoms	$t$	$\Delta\varepsilon$
V <sub>2a</sub> -V <sub>1a</sub>	0.070	0.135	V <sub>2a</sub> -V <sub>3a</sub>	-0.024	-0.022
V <sub>2b</sub> -V <sub>1b</sub>	0.094	-0.046	V <sub>2b</sub> -V <sub>3b</sub>	0.054	0.093

---

Inter-ladder Inter-IPN					
Atoms	$t$	$\Delta\varepsilon$	Atoms	$t$	$\Delta\varepsilon$
V <sub>3a</sub> -V <sub>3a'</sub>	0.023	0.002	V <sub>3a</sub> -V <sub>3b'</sub>	-0.053	-0.038
V <sub>3b</sub> -V <sub>3b'</sub>	-0.059	0.006	V <sub>3b</sub> -V <sub>3a-b</sub>	-0.053	-0.038

TABLE I: EHTB values of the hopping and vanadium magnetic orbital energies (eV).

- \* On leave to : Laboratoire CRISMAT / UMR 6508, 6 boulevard Marchal Juin, F-14050 Caen Cedex 4, FRANCE
- <sup>1</sup> M. Isobe and Y. Ueda, *J. Phys. Soc. Jnp.* **65**, 1178 (1996).
  - <sup>2</sup> M. Köppen, D. Pankert, R. Hauptmann, M. Lang, M. Weiden, C. Geibel, and F. Steglich, *Phys. Rev. B* **57**, 8466 (1998).
  - <sup>3</sup> T. Ohama, H. Yasuoka, M. Isobe and Y. Ueda, *Phys. Rev. B* **59**, 3299 (1999).
  - <sup>4</sup> B. Grenier, O. Cepas, L. P. Regnault, J. E. Lorenzo, T. Ziman, J. P. Boucher, A. Hiess, T. Chatterji, J. Jegoudez and A. Revcolevschi, *Phys. Rev. Letters* **86**, 5966 (2001).
  - <sup>5</sup> C. Presura, D. van der Marel, A. Damascelli and R.K. Kremer, *Phys. Rev. B* **61**, 15762 (2000).
  - <sup>6</sup> Y. Joly, S. Grenier and J.E. Lorenzo, *Phys. Rev. B* **68**, 144412 (2003).
  - <sup>7</sup> N. Suaud and M.-B. Lepetit, *Phys. Rev. Letters* **88**, 056405 (2002).
  - <sup>8</sup> H. Yamada and Y. Ueda, *J. Phys. soc. Jpn.* **68**, 2735 (1999).
  - <sup>9</sup> H. Yamada and Y. Ueda, *Physica B* **284**, 1651 (2000).
  - <sup>10</sup> Y. Ueda, H. Yamada, M. Isobe, T. Yamauchi, J. Alloys Compounds **317-318**, 109 (2001).
  - <sup>11</sup> Z. V. Popovic et al, *J. Phys. Condens. Matter* **15**, L139 (2003).

- <sup>12</sup> V. Ta Phuoc, private communication.
- <sup>13</sup> J. Ren ; W. Liang and M.-H. Whangbo *Crystal and Electronic Structure Analysis Using CAESAR* (1998) ; M.-H. Whangbo, H.-J. Koo and D. Dai, *J. Solid State Chem.* **176**, 417 (2003).
- <sup>14</sup> Cl. Sellier, Fl. Boucher, E. Janod, *Solid state sci.* **5**, 591 (2003).
- <sup>15</sup> N. Suaud and M.-B. Lepetit, *Phys. Rev. B* **62** 402 (2000).
- <sup>16</sup> Z. V. Popović, M. J. Konstantinović, R. Gajić, V. N. Popov, M. Isobe, Y. Ueda and V. V. Moshchalkov, *Phys. Rev. B* **65**, 184303 (2002).
- <sup>17</sup> J. Spitaler, E.Ya. Sherman, C. Ambrosch-Draxl, H.-G. Evertz, cond-mat/0401458.
- <sup>18</sup> P. H. M. van Loosdrecht, C. N. Presura, M. Popinciuc, D. van der Marel, G. Maris, T. T. M. Palstra, P. J. M. van Bentum, H. Yamada, T. Yamauchi, Y. Ueda, *J. supercond.* **15**, 587 (2002).
- <sup>19</sup> W. S. Bacsa, R. Lewandowska, A. Zwick, and P. Millet, *Phys. Rev. B* **61**, R14885 (2000).
- <sup>20</sup> E. Dagotto, J. Riera and D. Scalapino, *Phys. Rev. B* **45**, 5744 (1992); M. Sigrist, T. M. Rice and F. C. Zhang, *Phys. Rev. B* **49**, 12058 (1994); H. Tsunetsugu, M. Troyer and T. M. Rice, *Phys. Rev. B* **49**, 16078 (1994).